Food and Chemical Toxicology 129 (2019) 344–353

Contents lists available at ScienceDirect

Food and Chemical Toxicology

journal homepage: www.elsevier.com/locate/foodchemtox

Bee venom attenuates *Porphyromonas gingivalis* and RANKL-induced bone resorption with osteoclastogenic differentiation

Hyemin Gu[a], Hyun-Jin An[a], Jung-Yeon Kim[f], Woon-Hae Kim[b], Mi-Gyeong Gwon[a], Hyun-Ju Kim[a], Sang Mi Han[c], InSook Park[d], Sok Cheon Park[e], Jaechan Leem[f], Kwan-Kyu Park[a,*]

[a] Department of Pathology, School of Medicine, Catholic University of Daegu, 42472, Republic of Korea
[b] Department of New Biology, DGIST, Daegu, 42988, Republic of Korea
[c] Department of Agricultural Biology, National Academy of Agricultural Science, RDA, 54875, Republic of Korea
[d] Department of Oral and Maxillofacial Surgery, Department of Dentistry, School of Medicine, Catholic University of Daegu, 42472, Republic of Korea
[e] School of Biomedical Sciences, Charles Sturt University, Panorama Avenue, Bathurst, NSW, 2795, Australia
[f] Department of Immunology, School of Medicine, Catholic University of Daegu, 42472, Republic of Korea

Keywords:
Bee venom
Periodontal diseases
Osteoclastogenesis
Inflammation

A B S T R A C T

Porphyromonas gingivalis (*P. gingivalis*) is one of the major periodontal pathogens leading to inflammation and alveolar bone resorption. Bone resorption is induced by osteoclasts, which are multinucleated giant cells. Osteoclastic bone resorption is mediated by enhanced receptor activator of nuclear factor-kappa B ligand (RANKL) signaling. Therefore, the down-regulation of RANKL downstream signals is regarded as an effective therapeutic target in the treatment of bone loss-associated disorders. The aim of this study was to evaluate whether purified bee venom (BV) could attenuate *P. gingivalis*-induced inflammatory periodontitis and RANKL-induced osteoclast differentiation. Inflammatory periodontitis induced by *P. gingivalis* increased alveolar bone resorption and increased expression of TNF-α and IL-1β, while BV treatment resulted in decreased bone loss and pro-inflammatory cytokines. Similarly, RANKL-induced multinucleated osteoclast differentiation and osteoclast-specific gene expression, such as nuclear factor of activated T cells 1 (NFATc1), cathepsin K, tartrate-resistant acid phosphatase (TRAP), and integrin αvβ3 were significantly suppressed by treatment with BV. We show that BV reduces *P. gingivalis*-induced inflammatory bone loss-related periodontitis *in vivo* and RANKL-induced osteoclast differentiation, activation, and function *in vitro*. These results suggest that BV exerts positive effects on inflammatory periodontitis associated osteoclastogenesis.

1. Introduction

Periodontitis is a chronic disease of bacterial origin that destroys the tissue supporting teeth, including resorption of periodontal ligaments and alveolar bone. Periodontitis can cause not only tooth loss but also systemic diseases, such as cardiovascular disease and rheumatoid arthritis (Pizzo et al., 2010). Periodontitis is caused by the accumulation of the anaerobic gram-negative, non-motile bacterium, *Porphyromonas gingivalis* (*P. gingivalis*), which causes the destruction of periodontal tissue in the subgingival biofilm (Haffajee and Socransky, 1994).

P. gingivalis is present at sites with periodontal disease and is one of the most important pathogens associated with chronic periodontitis (Bhattarai et al., 2017; Cutler et al., 1995). *P. gingivalis* expresses a variety of virulence factors that contribute to survival in oral environments, such as lipopolysaccharides (LPS), fimbriae, hemagglutinins, and gingipains (Holt et al., 1999). These virulence factors can induce inflammatory responses to periodontal tissue and subsequent alveolar bone resorption by stimulating host cells, such as gingival macrophages and fibroblasts (Bhattarai et al., 2017; Holt et al., 1999). In addition, periodontal infection is accompanied by an initial inflammatory response that not only amplifies the host immune cells of the periodontal tissue but also induces bone resorption associated with inflammatory mediators, such as cytokines, chemokines and adhesion molecules (Geissmann et al., 2010).

Abbreviations: ABC, alveolar bone crest; BV, bee venom; CCK, cell counting kit; CEJ, cemento-enamel junction; DC-STAMP, dendritic cell-specific transmembrane protein; F-actin, filamentous actin; LPS, lipopolysaccharides; μ-CT, micro-computed tomography; NFATc1, nuclear factor of activated T cells 1; *P. gingivalis*, *Porphyromonas gingvalis*; RANKL, receptor activator of nuclear factor-kappa B; TRAP, tartrate-resistant acid phosphatase

* Corresponding author. Department of Pathology, School of Medicine, Catholic University of Daegu, 33, Duryugongwon-ro 17-gil, Nam-gu, Daegu, 42472, Republic of Korea.
E-mail addresses: kkpark@cu.ac.kr, guhm1207@cu.ac.kr (K.-K. Park).

https://doi.org/10.1016/j.fct.2019.05.001
Received 18 February 2019; Received in revised form 11 April 2019; Accepted 1 May 2019
Available online 02 May 2019

Bone resorption is induced by osteoclasts in patients with periodontitis (Cochran, 2008b). Osteoclasts are multinucleated giant cells derived from monocytes/macrophage lineage cells. Receptor activator of nuclear factor-kappa B ligand (RANKL) is a key regulator of osteoclast function and survival. It binds to RANK receptors on the surface of osteoclast precursors and induces osteoclast differentiation by activating nuclear factor of activated T cells 1 (NFATc1), a transcription factor essential for osteoclastogenesis (Boyce, 2013; Lacey et al., 1998; Takayanagi et al., 2002). The activated NFATc1 regulates a variety of genes essential for osteoclast differentiation and function, such as tartrate-resistant acid phosphatase (TRAP), cathepsin K, and dendritic cell-specific transmembrane protein (DC-STAMP) (Li et al., 2006; Yagi et al., 2005). Osteoclasts are known to secrete cathepsin K during bone resorption, and cathepsin K is a lysosomal cysteine protease that acts as a major enzyme in activating TRAP and degrading bone matrix proteins (Fuller et al., 2008; Zenger et al., 2007). Some studies have shown that osteoclasts are unable to resorb the bone mineral matrix in the state of cathepsin K deficiency (An et al., 2016; Wilson et al., 2009). TRAP is a phenotypic marker of osteoclast differentiation and exhibits bone resorption activity in lysosomes that are highly expressed in osteoclasts (Halleen et al., 1999). Matrix metalloproteinase (MMP)-9 secreted by osteoclasts is a protease that causes bone resorption and destruction of the collagen matrix. It is known that MMP-9 promotes osteoclast migration and is involved in the osteoclast bone resorption process (Ishibashi et al., 2006). DC-STAMP plays an essential role in the fusion of mononuclear osteoclasts (Zhang et al., 2014a).

Structural reconstruction of the actin ring composed mainly of filamentous actin (F-actin) is a characteristic cytoskeletal structure of functional osteoclasts. Bone resorption occurs only when the sealing zone is formed by an actin ring structure (An et al., 2016). The sealing zone, which is composed of F-actin, plays an important role in osteoclast adhesion to the bone surface through the expression of integrin αv and β3 (Väänänen and Horton, 1995). Integrin $\alpha v\beta 3$, membrane glycoproteins of heterodimers composed of α and β subunits, are cell surface receptors that regulate cell-cell and cell-matrix interactions. This integrin-modulated signaling plays an important role in regulating a variety of cellular functions, including bone resorption (Nakamura et al., 2007b).

When the binding of RANKL and RANK on osteoclast precursor cells occurs, it induces the activation of tumor necrosis factor receptor-associated factor 6 (TRAF6) (Kobayashi et al., 2001), NF-κB, and mitogen-activated protein kinases (MAPKs), such as extracellular signal-regulated kinase 1/2 (ERK 1/2), p38, and c-Jun N-terminal kinase (JNK) (Hotokezaka et al., 2002; Matsuo et al., 2004). In addition, inflammatory cytokines, such as interleukin (IL)-6, IL-1β, and tumor necrosis factor (TNF)-α, are involved in the pathogenesis of periodontal disease (Zhou et al., 2005).

The treatment of periodontitis often involves mechanical procedures and antibiotic administration. However, this lacks strategies that directly address the immune aspects of the disease (Cochran, 2008a). Therefore, this study suggests that a therapeutic approach is needed to target specific factors related to periodontal disease.

Purified bee venom (BV) is a natural toxin produced by honeybees (*Apis mellifera* L.). BV is composed of several active peptides, including melittin, apamin, adolapin, mast cell-degranulating peptides, and enzymes (Habermann, 1972; Hider, 1988). BV has been used in treating inflammatory diseases such as rheumatoid arthritis, skin diseases, and back pain (Kwon et al., 2001, 2002; Stieger et al., 1978). The anticancer properties of BV have also been demonstrated in hepatocellular carcinoma cells, lung cancer cells, prostate cancer cells, and breast cancer cells (Ip et al., 2008; Orsolic, 2012; Park et al., 2011). However, there has not yet been a robust attempt to validate the therapeutic effects of BV in periodontitis. For this reason, this study evaluated the anti-inflammatory and anti-periodontitis effect of BV as an alternative to periodontitis treatment.

The current study established osteoclastogenic differentiation by RANKL treatment in a mouse monocyte/macrophage cell line *in vitro* and a periodontal animal model induced by the administration of *P. gingivalis* in mice *in vivo*. The effects of BV on osteoclastogenic differentiation and function by RANKL were investigated. Furthermore, the bone resorption after BV administration was evaluated in *P. gingivalis*-induced periodontal disease animal model.

2. Materials and methods

2.1. Bee venom collection

The colonies of natural honeybees (*Apis mellifera* L.) used in the present study were maintained at the National Institute of Agricultural Science and Technology (Suwon, Korea). BV was collected using the collecting device (Chung Jin Biotech Co., Ltd., Ansan, Korea) in a sterile manner under strict laboratory conditions. In brief, the BV collector was placed in the hive, and the bees were given enough electric shock to cause them to sting a glass plate from which dried BV was later scraped off. The collected BV was purified by the methods of Han et al. (2016). In brief, the collected BV was diluted in cold water and then centrifuged at 10,000 g for 5 min at 4 °C to discard residues from the supernatant. BV was lyophilized by freeze dryer and refrigerated at 4 °C for later use. The BV used in the experiment was confirmed with size exclusion gel chromatography (AKTA Explorer; GE Healthcare, Pittsburgh, PA, USA) by dissolving in 0.1 M ammonium formate adjusted to pH 4.5. A Sephadex TM75 column (Amersham Biosciences, Piscataway, NJ, USA) with further purification by a Source 15RPC ST column (GE Healthcare, Little Chalfont, UK) with 0.1% trifluoracetic acid in 20% acetonitrile as the eluent was used to confirm the presence of melittin, the major active ingredient of BV.

2.2. Bacteria

P. gingivalis strain KCTC 5352 was grown anaerobically at 37 °C in tryptic soy broth (MB Cell, Los Angeles, CA, USA) supplemented with 5 μg ml^{-1} hemin, 2.5 μg ml^{-1} menadione, 5% sheep's blood, and 1.5% agar. The concentration of bacteria was standardized with a spectrophotometer to an optical density of 1 at 600 nm, which corresponds to 10^9 colony forming units (CFU) of live *P. gingivalis* per ml. Then, 10^9 CFU ml^{-1} of bacteria were suspended in 20 μl of phosphate buffered saline (PBS) with 2% carboxymethylcellulose (CMC, Sigma-Aldrich, St. Louis, MO, USA). We used an inoculation concentration of 10^9 CFU ml^{-1} based on our preliminary data showing alveolar bone loss following the bacterial invasion of the periodontium.

2.3. Murine model of alveolar bone loss

Six-week old male Balb/C mice (n = 30) were purchased from Samtako (Osan, Korea) and housed at 55% humidity and 22 ± 2 °C in a 12-h light-dark cycle and allowed food and water ad libitum for 7 days. The mice were randomly divided into 5 groups; normal control (NC group), *P. gingivalis* injection (P. g group), and *P. gingivalis* with 1, 10, 100 μg BV per kg of bodyweight (BV1, BV10, and BV100 group). The mice were put under brief isoflurane anesthesia, and 10^9 CFU *P. gingivalis* in 20 μl of PBS with 2% CMC was applied to the gingival margin between the first and second maxillary molar sections. The mice in the NC group received 20 μl of PBS with 2% CMC. The experimental period for establishing *P. gingivalis*-induced periodontal animal models was 7 weeks. *P. gingivalis* was given twice a week for 3 weeks, and then for 4 weeks BV and *P. gingivalis* were administered once a week on different days each. The mice were sacrificed by CO_2 asphyxiation, and their maxillary specimens were excised for micro-CT and histomorphometry. Isolated mice maxillary tissues were fixed in 3.7% formaldehyde for one day, decalcified in 10% EDTA for 2 weeks, and embedded in paraffin. Animal care and all experimental procedures were approved and conducted in accordance with the guidelines of the Institutional Animal

Care and Use Committee of the Catholic University of Daegu (Approval number: DCIAFCR-170105-12-Y).

2.4. Cell culture and osteoclast differentiation

Mouse monocyte/macrophage RAW 264.7 cells were purchased from American Type Culture Collection (Manassas, VA, USA). RAW 264.7 cells were grown in Dulbecco's modified Eagle's medium (DMEM) supplemented with 10% fetal bovine serum (FBS) and 1% antibiotics. All cells were cultured in a humidified atmosphere containing 5% CO_2 at 37 °C. To induce osteoclastogenesis, RAW 264.7 cells were seeded at 5×10^4 cells ml^{-1} and cultured in DMEM for 24 h. The cells were then treated with DMEM medium containing 100 ng ml^{-1} soluble RANKL (PeproTech, Rocky Hill, NJ, USA) in the presence or absence of different concentrations of BV (1, 10, and 100 ng ml^{-1}) for 5 days. The growth medium containing RANKL and BV was replaced on day 3.

2.5. Cell viability assay

The cell viability of RAW 264.7 was determined using the cell counting kit (CCK)-8 assay (Dojindo, Kumamoto, Japan). The cells were seeded in a 96-well plate at 5×10^2 cells per well and pre-incubated for 24 h. After pre-incubation, the cells were treated with various concentrations of BV for 5 d. After treatment, 10 μl of WST-8 solution [2-(2-methoxy-4-nitrophenyl)-3-(4-nitrophenyl)-5-(2,4-disulfophenyl)-2H-tetrazolium, monosodium salt] was added to each well, and the cells were incubated for an additional 4 h at 37 °C. The cell viability values were measured by absorbance at 450 nm using a microplate reader.

2.6. Western blot analysis

Protein samples were extracted from the cultured RAW 264.7 cells with a lysis buffer (Cell Lytic™ M; Sigma-Aldrich). After incubation for 30 min on ice, the total extract was centrifuged at 12,000 rpm at 4 °C for 10 min and the supernatant was collected. The protein concentration of the samples was measured using a Bradford assay (Bio-Rad Laboratories, Hercules, CA, USA) at 595 nm, by using a spectrophotometer. Protein samples were separated using precast gradient polyacrylamide gels (Bolt™ 4–12% Bis-Tris Plus Gels; Thermo Fisher Scientific, Waltham, MA, USA), transferred to nitrocellulose membrane (GE Healthcare, Chicago, IL, USA). The membrane was blocked in 5% bovine serum albumin. Membranes were probed with primary antibodies and horseradish peroxidase-conjugated secondary antibody. Signal intensity was measured with an image analyzer (ChemiDoc™ XRS+; Bio-Rad Laboratories) and quantified using Image Lab software (Bio-Rad Laboratories). The protein expression values were normalized to β-actin (Sigma-Aldrich) expression values. The primary antibodies used were as follows: anti-NFATc1 (BD Pharmingen, San Diego, CA, USA), anti-integrin-αv, anti-integrin-β3, anti-ERK, anti-phospho-ERK, anti-JNK, anti-phospho-JNK, anti-p38, anti-phospho-p38 (Cell Signaling Technology, Danvers, MA, USA), anti-IL-8, anti-IL-1β, cathepsin K (Santa Cruz Biotechnology, Dallas, TX, USA), anti-TNF-α (Abcam, Cambridge, Cambridgeshire, UK), and anti-β-actin (Sigma-Aldrich).

2.7. Tartrate-resistant acid phosphatase (TRAP) staining

The osteoclast activity was detected by osteoclast marker protein TRAP staining using Leukocyte Acid Phosphatase Assay kit (Sigma-Aldrich). For osteoclast differentiation, the RAW 264.7 cells were seeded in 6-well plates at a density of 3×10^4 cells ml^{-1}. They were then cultured in the presence of RANKL and different concentrations of BV (1, 10 and 100 ng ml^{-1}) for 5 days. The culture medium was replaced on day 3. After the completion of differentiation, the cells were fixed and stained according to the manufacturer's instructions. Briefly, cells were washed with PBS and fixed with 3.7% formaldehyde for 10 min. After washing with PBS, cells were incubated with 0.1% (v/v) Triton X-100 for 1 min. Cells were washed, and then incubated for 1 h at 37 °C in the dark with a mixture of solutions of Fast Garnet GBC, sodium nitrite, naphthol AS-BI phosphoric acid, acetate, and tartrate from the Leukocyte Acid Phosphatase Assay kit. The cells were washed with distilled water, and TRAP-positive multinucleated cells containing three or more nuclei were counted.

Tissues embedded in paraffin were cut into 4 μm thick sections. For histological examination, the sections were stained with TRAP according to the manufacturer's instructions. All slides were examined under a Pannoramic MIDI slide scanner (3DHISTECH, Budapest, Hungary).

2.8. Immunofluorescence analysis

RAW 264.7 cells were stimulated with RANKL (100 ng ml^{-1}) for 5 days to induce osteoclast differentiation in the presence or absence of BV (1, 10, and 100 ng ml^{-1}). To detect acidic lysosomes, cells were incubated for 30 min with 40 nM acidotropic probe LysoTracker Deep Red (Life Technologies, Carlsbad, CA, USA). Cells were fixed with 3.7% formaldehyde for 15 min and permeabilized with 0.1% Triton X-100 for 5 min. Following permeabilization, the cells were incubated for 20 min with Alexa Fluor 488 phalloidin (Thermo Fisher Scientific) for double staining of the F-actin rings. The nuclei were stained with Hoechst 33342 solution for 20 min. The slides were mounted using a fluorescence mounting medium (Dako, Santa Clara, CA, USA). Fluorescent images were obtained with a confocal microscope system A1 (Nikon, Tokyo, Japan).

2.9. Micro-computed tomography (μ-CT) analysis

Micro-CT imaging of mice maxillae was performed using Quantum FX micro-CT (PerkinElmer, Massachusetts, USA). The X-ray source was set at 90 kVp and 180 μA with a field of view of 5 mm. After rotating and adjusting the image using RadiAnt DICOM software, the distance from the cemento-enamel junction (CEJ) to the alveolar bone crest (ABC) was measured to assess bone resorption.

2.10. Histologic analysis

The maxillary specimens were fixed in 10% neutral buffered formalin for at least 24 h at room temperature and were subjected to 2 weeks decalcification in 10% EDTA. The maxillary specimens were dissected, dehydrated, and embedded in paraffin. Thereafter, thin sections (4 μm) were mounted on glass slides and stained with hematoxylin and eosin (H&E). All slides were examined under a Pannoramic® MIDI slide scanner (3DHISTECH).

2.11. Immunohistochemical analysis

The paraffin-embedded tissue sections on slides were deparaffinized. The sections were then incubated with a primary antibody for 1 h at 37 °C. The primary antibodies were anti-TNF-α (Abcam) and anti-IL-1β (Santa Cruz Biotechnology). The signal was visualized using an Envision System (DAKO) for 30 min at 37 °C; 3,3′-diaminobenzidine tetrahydrochloride was used as the coloring reagent, and hematoxylin was used as the counter-stain. The slides were examined with a Pannoramic® MIDI slide scanner, and the integrated optical density was analyzed with i-Solution DT software.

2.12. Statistical analysis

All data are presented as means ± standard deviation (SD). Statistical significance was tested by one-way analysis of variance with a Tukey's multiple comparison test. Differences with $p < 0.05$ were considered significant.

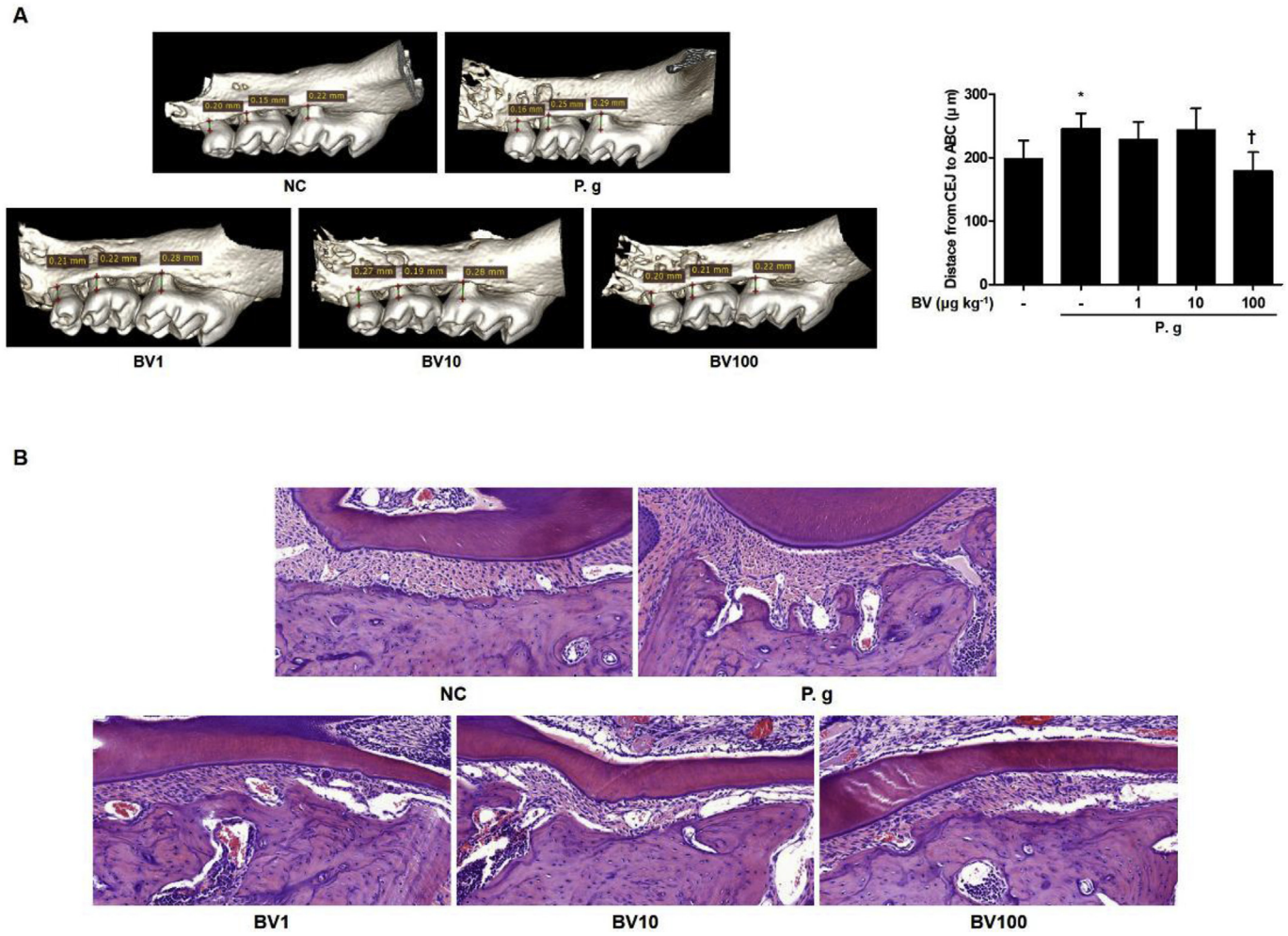

Fig. 1. Effect of BV on alveolar bone loss and histological damage induced by *P. gingivalis*.

3. Results

3.1. BV attenuates P. gingivalis-induced bone resorption

Alveolar bone resorption was analyzed by forming a 3-dimensional (3D) structure using a highly sensitive and accurate micro-CT scanner to investigate and evaluate bone loss in animal model. The 3D reconstruction of the maxilla represents the palatal surface of the alveolar bone and the length of bone loss from the CEJ to the ABC parameters represents the difference between groups by marking three spots. Micro-CT analysis demonstrated that the alveolar bone process distance was greater in the *P. gingivalis* group relative to NC group (Fig. 1A), indicating that *P. gingivalis* led to higher bone loss. The administration of high dose of BV significantly decreased the distance of alveolar bone process. H&E staining analysis demonstrated that *P. gingivalis* induced the occurrence of osteolytic lesions in the periodontal tissue, whereas osteolytic lesions were alleviated with BV treatment (Fig. 1B). These results show that *P. gingivalis* has the ability to cause periodontal tissue disruption and that BV is a potent mediator to prevent *P. gingivalis*-mediated periodontal disease progression.

(A) A representative micro-CT image of the maxilla of each group. The distance between the cemento-enamel junction (CEJ) and the alveolar bone crest (ABC) was measured. Data are expressed mean ± SD. One-way ANOVA was used to determine statistical significance. $^{*}p < 0.05$ compared to the NC group; $^{\dagger}p < 0.05$ compared to the P. g group. (B) Maxilla sections were stained using hematoxylin and eosin (H&E). Histological examinations were performed at 400 × magnification. NC: normal control; P. g: *P. gingivalis*; BV: 1, 10, and 100 μg kg^{-1} BV with *P. gingivalis*.

3.2. BV attenuates osteoclast formation and induction of pro-inflammatory cytokines in the inflamed region of mice with periodontitis

Osteoclasts are the only cells with bone resorption process *in vivo*. This study evaluated the formation of osteoclasts in gingival tissue. The formation of TRAP-positive multinucleated osteoclast cells increased in the *P. gingivalis*-infected group. On the other hand, treatment with BV reduced the formation of TRAP-positive multinucleated osteoclasts (Fig. 2A).

To determine the effect of BV on the expression of pro-inflammatory cytokines that influence bone resorptio, such as TNF-α and IL-1β, the gingival tissue sections were stained with TNF-α and IL-1β antibodies. The expression of TNF-α and IL-1β was increased in *P. gingivalis*-infected mice, while their expression was decreased by BV (Fig. 2B). These data suggest that BV can inhibit *P. gingivalis*-induced bone loss and the expression of pro-inflammatory cytokines *in vivo*.

(A) Tartrate-resistant acid phosphatase (TRAP) staining was performed to measure cells such as multinucleated osteoclasts on the alveolar bone surface. (B) Representative immunohistochemical analysis using TNF-α and IL-1β antibodies shows that BV decreased the expression of pro-inflammatory cytokines (in brown color) in periodontal tissues. Histological examinations were performed at 400 × magnification. Results are expressed as means ± SD. $^{*}p < 0.05$ compared to the NC group; $^{\dagger}p < 0.05$ compared to the P. g group. NC: normal

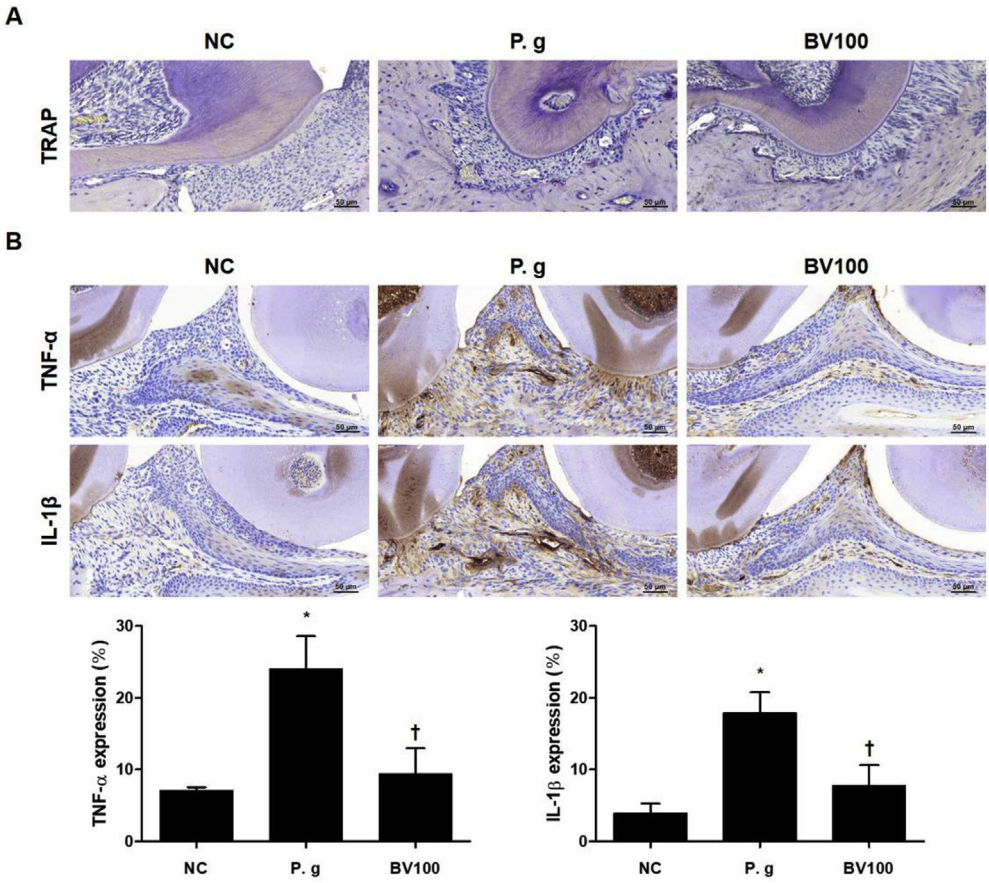

Fig. 2. Effect of BV on multinucleated osteoclast formation and pro-inflammatory cytokines by *P. gingivalis* in periodontal tissues.

control; P. g: *P. gingivalis*; BV: 100 μg kg^{-1} BV with *P. gingivalis*.

3.3. BV shows no cytotoxic effect in RAW 264.7 cells

We first determined the toxicity of BV in RAW 264.7 cells. The treatment of RAW 264.7 cells with 1, 5, 10, 50, and 100 ng ml^{-1} of BV for 5 days did not affect cell viability (Fig. 3A). Therefore, the following experiments were performed using BV concentrations of 1, 10, and 100 ng ml^{-1}.

(A) Cellular toxicity of BV was assessed using the CCK-8 method. The optical density was measured at 450 nm. (B) Whole cell lysates were subjected to SDS-PAGE and Western blotting with specific antibodies against NFATc1, integrin αv, integrin β3, cathepsin K, TNF-α, IL-1β and IL-8. (C-E) The graph represents the bands normalized to β-actin. All gels were run under identical experimental conditions. The results are expressed as means ± SD of three independent experiments. One-way ANOVA was used to determine statistical significance. $^{*}p < 0.05$ compared to the NC group; $^{\dagger}p < 0.05$ compared to the RANKL group. NC: normal control; RANKL: 100 ng ml^{-1} RANKL only; BV: 1, 5, 10, 50, and 100 ng ml^{-1} BV with RANKL.

3.4. BV inhibits RANKL-induced osteoclast-specific gene expression

Next, we examined in more detail the effect of BV on osteoclast-associated gene expression induced by RANKL in RAW 264.7 cells. RANKL-induced osteoclastogenesis is related to changes in the expression of osteoclast-specific genes. RANKL-stimulated expression of NFATc1, integrin αv, integrin β3, and cathepsin K genes was up-regulated in RAW 264.7 cells compared to the expression in normal control. We confirmed the inhibitory activity of BV (100 ng ml^{-1}) on the RANKL-induced expression of these genes (Fig. 3B–F). It was found that BV is able to negatively modulate the expression of genes involved in RANKL-induced osteoclastogenesis.

3.5. BV inhibits RANKL-induced pro-inflammatory cytokines

Pro-inflammatory cytokines such as TNF-α and IL-1β stimulate osteoclast differentiation and activation, resulting in bone resorption (Boyce, 2013; Taguchi et al., 2015). To further evaluate the mechanism underlying BV involvement in the regulation of cytokine secretion during osteoclastogenesis, the current study analyzed the expression of TNF-α and IL-1β in RAW 264.7 cells following RANKL stimulation. As shown in Fig. 3B, the level of TNF-α and IL-1β in the RAW 264.7 cells increased in response to RANKL relative to normal control. However, treatment with BV effectively decreased TNF-α and IL-1β levels in the monocyte/macrophage cell line.

3.6. BV inhibits RANKL-induced osteoclastogenic differentiation

The mouse monocyte/macrophage cell line RAW 264.7 has been shown to differentiate into osteoclasts upon exposure to RANKL (Boyce, 2013). The effect of BV on RANKL-induced osteoclast differentiation of RAW 264.7 cells was evaluated using TRAP staining, as TRAP is a well-known histochemical marker enzyme. Cells were incubated with BV in the presence of RANKL (100 ng ml^{-1}) for 5 days. In the absence of BV, RAW 264.7 cells differentiated into TRAP-positive multinucleated osteoclasts, while BV (1, 10, and 100 ng ml^{-1}) reduced the formation and number of TRAP-positive multinucleated osteoclasts in a dose-dependent manner (Fig. 4).

RAW 264.7 cells were cultured with an indicated concentration of BV in the presence of RANKL for 5 days. BV suppresses RANKL-induced osteoclast differentiation in a dose-dependent manner. The number of

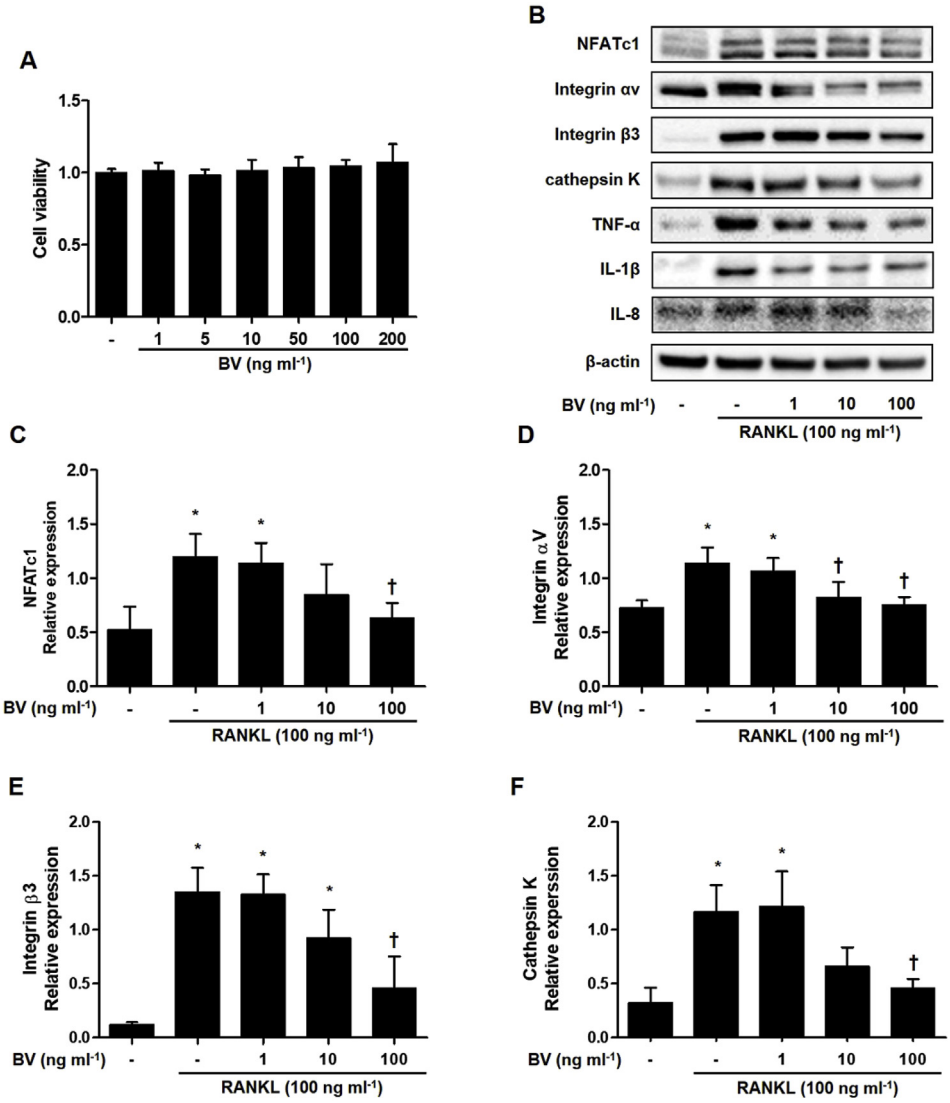

Fig. 3. Effect of BV on the expression of RANKL-induced osteoclastogenic markers and pro-inflammatory cytokines.

TRAP-positive cells containing more than three nuclei was counted at 200 × magnification, and the results expressed as the number of cells field of vision. Data are represented as means ± SEM of three independent experiments. One-way ANOVA was used to determine statistical significance. $^{*}p < 0.05$ compared to the NC group; $^{\dagger}p < 0.05$ compared to the RANKL group. NC: normal control; RANKL: 100 ng ml^{-1} RANKL only; BV: 1, 10, and 100 ng ml^{-1} BV with RANKL.

3.7. BV attenuates F-actin ring formation and osteoclast resorptive activity

Actin ring formation following the rearrangement of the cytoskeleton is a characteristic of highly activated osteoclasts (Boyle et al.,

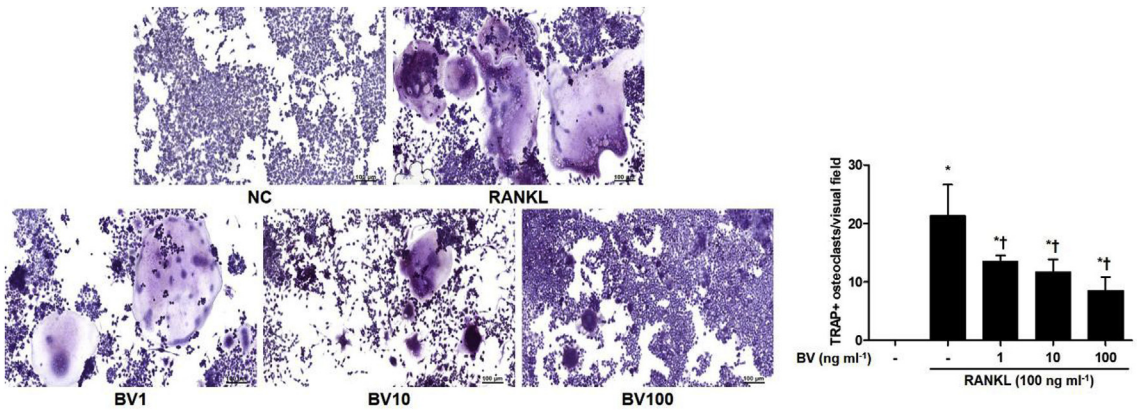

Fig. 4. Effect of BV on RANKL-induced osteoclastogenesis in RAW 264.7 cells.

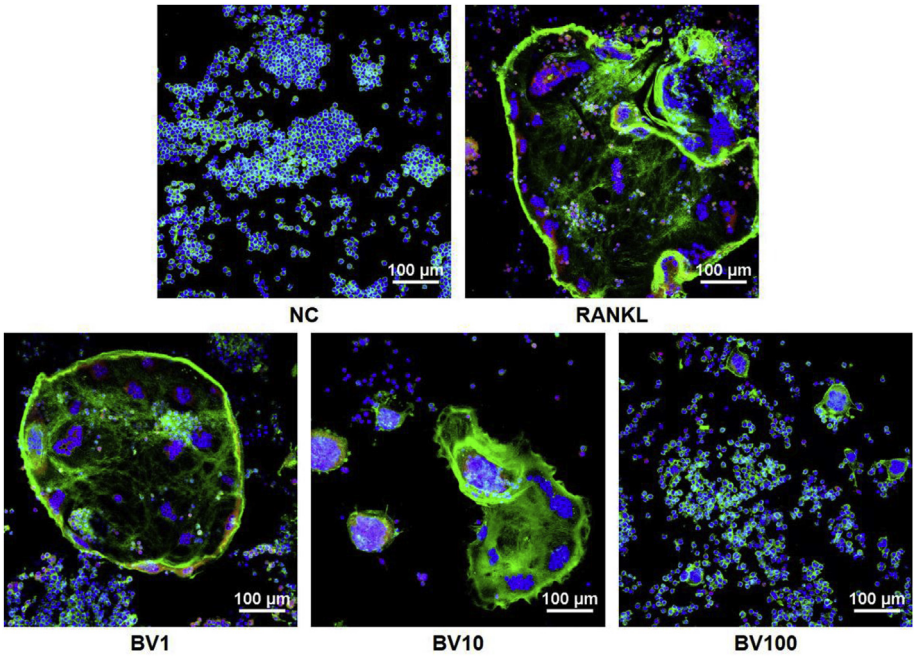

Fig. 5. Effect of BV on RANKL-induced actin ring formation and osteoclast resorptive activity in RAW 264.7 cells.

2003), and cathepsin K in osteoclasts is a lysosomal cysteine protease that plays an essential role in bone resorption (Turk et al., 2012). The effect of BV on the actin ring formation and osteoclast resorptive activity in RANKL-stimulated RAW 264.7 cells was investigated. The greenish staining of phalloidin resulted in notable increase in the formation of actin rings in RANKL-treated cells relative to normal controls. Similarly, the reddish staining of LysoTracker showed that the cathepsin K expression of lysosomal cysteine protease was markedly increased in RANKL-treated cells compared with normal control (Fig. 5). In contrast, the size and number of actin rings decreased in BV-treated cells compared with RANKL only cells. The expression of lysosomal cysteine protease also decreased with BV treatment in a dose-dependent manner. These findings suggest that BV inhibits osteoclastogenesis involved in bone loss by decreasing the formation of actin rings involved in bone resorption and of cathepsin K involved in bone matrix degradation.

RAW 264.7 cells were cultured with an indicated concentration of BV in the presence of 100 ng ml^{-1} RANKL for 5 days. For the staining of the actin ring and lysosomes, green Alexa Fluor 488-phalloidin and red fluorescent LysoTracker were used in differentiated cells, respectively. The nuclei were labeled with Hoechst 33342 (blue). Images are representative of at least three to five experiments. NC: normal control; RANKL: 100 ng ml^{-1} RANKL only; BV: 1, 10, and 100 ng ml^{-1} BV with RANKL.

3.8. BV suppresses RANKL-induced MAPKs signaling pathways

RANKL activates TRAF6 via RANK (Kobayashi et al., 2001) and subsequently triggers the activation of a series of MAPKs including Akt, ERK 1/2, p38, and JNK, that play an important role in early osteoclast differentiation (Matsumoto et al., 2000). To obtain greater insight into the molecular mechanisms by which BV inhibits osteoclastogenesis, the phosphorylation of Akt, ERK 1/2, p38, and JNK in RANKL-stimulated RAW 264.7 cells was examined using Western blotting. As shown in Fig. 6, RANKL treatment increased the phosphorylation of Akt, ERK 1/2, p38, and JNK. However, BV treatment (particularly the 100 ng ml^{-1} dose) decreased the phosphorylation levels of Akt, ERK 1/2, p38, and JNK (Fig. 6).

RAW 264.7 cells were pre-treated with the indicated concentrations

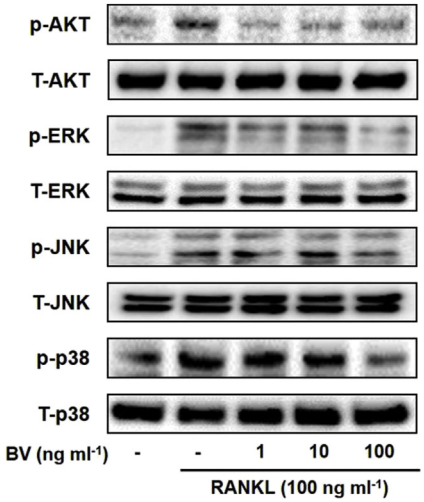

Fig. 6. Effect of BV on RANKL-induced MAPK signaling activity in RAW 264.7 cells.

of BV (1, 10, and 100 ng ml^{-1}) for 2 h, and then stimulated with 100 ng ml^{-1} RANKL for 10 min. Total protein extracts were analyzed by Western blotting using antibodies against phospho-Akt, total-Akt phospho-ERK, total-ERK, phospho-JNK, total-JNK, phospho-p38, and total-p38. NC: normal control; RANKL: 100 ng ml^{-1} RANKL only; BV: 1, 10, and 100 ng ml^{-1} BV with RANKL.

4. Discussion

BV is a natural toxin produced by honey bees and plays a major role in the defense of bee habitats (An et al., 2015; Orsolic, 2012; Son et al., 2007). As a traditional alternative medicine approach, BV has been used for centuries as an analgesic to reduce pain and as an anti-inflammatory agent for several inflammatory diseases (Billingham et al., 1973; Kim et al., 2015; Lee et al., 2015). Interestingly, BV has been reported to enhance the inflammatory response at relatively high concentrations (≥ 2.5 μg ml^{-1}) (Dombrowski et al., 2012), while exhibiting anti-inflammatory effects at relatively low concentrations

($\leq 100\ ng\ ml^{-1}$) (Kim et al., 2015; Lee et al., 2011). These results show that the anti-inflammatory effect of BV occurs at relatively low concentrations. Therefore, relatively low concentrations of BV were used in this study. In a previous study, Kim et al. reported that BV inhibits pro-inflammatory cytokines in *P. gingivalis* LPS-induced keratinocytes (Kim et al., 2016b). However, the mechanism of BV in attenuating bone loss and osteoclastogenesis of periodontal disease has not been clarified.

P. gingivalis is one causative bacteria of periodontal disease (Cutler et al., 1995). It is commonly found in periodontal pockets of patients with chronic periodontitis (Bougas et al., 2013) and causes an inflammatory reaction that invades the gingival tissue and leads to alveolar bone destruction (Garlet, 2010; Liu et al., 2010a). The *P. gingivalis* infection model has been widely used to study immune-mediated gingival bone resorption (Han et al., 2013). Several studies have reported that clinically infected periodontal tissues are associated with an increase in the number of *P. gingivalis* bacteria and increased RANKL levels (Sakellari et al., 2008; Wara-aswapati et al., 2007). Therefore, we demonstrated the effect of BV on alveolar bone loss using *P. gingivalis*-induced periodontitis mouse model and the effect of BV on RANKL-induced osteoclastogenesis *in vitro*.

In this study, micro-CT analysis showed that alveolar bone loss was higher in the periodontitis mouse model and that it decreased in the mice treated with BV. Similar to other animal studies (Li and Amar, 2007; Zhang et al., 2014b), the histologic analysis showed the expression of pro-inflammatory cytokines, increased osteoclast formation, and bone loss by *P. gingivalis* infection. On the other hand, osteoclast formation and alveolar bone loss caused by *P. gingivalis* were inhibited after BV-treatment. In addition, several studies have reported that inflammatory mediators of the host infected with *P. gingivalis* are associated with gingival tissue destruction and alveolar bone loss, while anti-inflammatory mediators inhibit and attenuate disease progression (Garlet, 2010; Han et al., 2013; Liu et al., 2010b). These studies suggest that pro-inflammatory cytokines may play an important role in the *P. gingivalis*-induced alveolar bone loss. In this study, the up-regulation of pro-inflammatory cytokines such as TNF-α and IL-1β, which contribute to alveolar bone loss was shown to be down-regulated after BV treatment. Therefore, these results suggest that BV has a beneficial effect on alveolar bone loss *in vivo*.

RANKL, a key regulator of mature osteoclast function and survival, induces osteoclast differentiation by binding to the receptor RANK on the surface of osteoclast precursors (Lacey et al., 1998; Takayanagi et al., 2002). The role of osteoclasts in periodontal disease is known to cause alveolar bone destruction (Cochran, 2008a; Hajishengallis, 2014). Therefore, RANKL was used to induce osteoclastogenic differentiation in this study. Furthermore, RANK-RANKL binding induces the activation of MAPKs (ERK 1/2, p38, and JNK), leading to osteoclast-specific gene expression such as integrin αv, integrin β3, and cathepsin K (Kong et al., 2015). Downstream of RANKL signaling, MAPKs have been implicated as major regulators of various cellular responses, including cell proliferation, differentiation and apoptosis (Kim et al., 2013; Sui et al., 2014). MAPKs also play a pivotal role in the development of osteoclasts and have been considered potential molecular targets in inflammatory bone diseases, such as periodontal disease (Thummuri et al., 2015). In the current study, pre-treatment with BV was observed to reduce the phosphorylation of Akt, ERK1/2, p38, and JNK by RANKL. Based on these results, it is suggested that BV treatment could target the Akt, ERK 1/2, p38, and JNK cascades. Furthermore, several studies have shown that NFATc1 is an important transcription factor for RANKL-mediated osteoclast differentiation, fusion, and activation (Choi et al., 2010; Zhao et al., 2010). NFATc1, which acts as a downstream effector of RANKL, is known to regulate gene expression involved in osteoclast differentiation and function, such as TRAP, cathepsin K, integrin αv, and integrin β3 (Kim et al., 2014, 2016a). We adopted RANKL-induced osteoclastogenic differentiation platform from RAW 264.7 cells to analyze molecular mechanisms. BV affects not only the expression of NFATc1 but also downstream gene expression. The expression of pro-inflammatory cytokines was also inhibited by BV *in vitro*. These results suggest that BV could inhibit osteoclastogenesis.

It is important that the sealing zone of the periodontal tissue forms before mature osteoclasts are attached to the extracellular bone matrix for the purpose of bone destruction (Cremasco et al., 2012). The sealing zone, which is composed mainly of F-actin, plays an important role in the adhesion of osteoclasts to the bone surface through the expression of integrin αν and β3 (Cremasco et al., 2012; Nakamura et al., 2007a). The bone resorption function of osteoclasts is regulated by the lysosomal cysteine protease cathepsin K (Turk et al., 2012). Several studies have reported that the inhibition of integrin αv, β3, and F-actin ring formation results in the inhibition of osteoclast function (Baek et al., 2015; Mau et al., 2016). We investigated the effects of expressions of integrin αv and β3, the formation of the F-actin ring, and bone resorption to determine the role of BV in RANKL-induced osteoclastogenesis. As expected, BV inhibited integrin αv and integrin β3, F-actin ring formation, and lysosomal cysteine protease in a dose-dependent manner. Therefore, BV was effective in inhibiting the formation of osteoclasts and the activity of cathepsin K. This study also investigated osteoclastogenesis through TRAP staining in RAW 264.7 cells. TRAP staining showed that RANKL-induced osteoclastogenesis decreased after BV treatment in a dose-dependent manner. Therefore, BV has been shown to be effective in inhibiting osteoclastogenic differentiation and bone resorption capability. These results suggest that BV could prevent diseases associated with bone loss, such as periodontal disease.

5. Conclusions

BV attenuates alveolar bone loss in model of periodontal disease induced by *P. gingivalis in vivo* and inhibits osteoclastogenic differentiation induced by RANKL *in vitro*. *P. gingivalis* invades the periodontal tissue and causes an increase in osteoclast formation. The increased osteoclast formation by *P. gingivalis* has been shown to be inhibited by BV treatment. In addition, the expression of increased pro-inflammatory cytokines by *P. gingivalis* infection in periodontal tissue has been shown to be reduced through BV treatment. These results suggest that BV might have a protective effect against periodontal disease. Based on the results of the periodontal disease model, we determined the effect of BV on osteoclastogenic differentiation induced by RANKL *in vitro*. The expression of MAPKs and NFATc1 activated by RANK-RANKL binding affects a variety of cellular responses, including cell proliferation and differentiation. Furthermore, MAPKs and NFATc1 increased the expression of various osteoclast-specific genes, such as cathepsin K, integrin αv, and integrin β3. However, the activation of MAPKs and NFATc1 were inhibited by BV treatment. This study showed that the expression of various osteoclast-specific genes was significantly decreased through the inhibition of NFATc1 and MAPK signaling. The results show that BV can attenuate alveolar bone destruction by direct inhibition of RANKL-stimulated osteoclast differentiation, activation, and function. Therefore, this study suggests the potential for BV to prevent osteoclast-related diseases such as periodontal disease.

Declaration of interests

The authors declare that they have no known competing financial interests or personal relationships that could have appeared to influence the work reported in this paper.

The authors declare the following financial interests/personal relationships which may be considered as potential competing interests:

Acknowledgements

This work was carried out with the support of “Cooperative Research Program for Agriculture Science & Technology Development (Project No. PJ01316601)” Rural Development Administration,

Republic of Korea.

Appendix A. Supplementary data

Supplementary data to this article can be found online at https://doi.org/10.1016/j.fct.2019.05.001.

References

An, H.J., Kim, K.H., Lee, W.R., Kim, J.Y., Lee, S.J., Pak, S.C., Han, S.M., Park, K.K., 2015. Anti-fibrotic effect of natural toxin bee venom on animal model of unilateral ureteral obstruction. Toxins 7, 1917–1928.

An, J., Hao, D., Zhang, Q., Chen, B., Zhang, R., Wang, Y., Yang, H., 2016. Natural products for treatment of bone erosive diseases: the effects and mechanisms on inhibiting osteoclastogenesis and bone resorption. Int. Immunopharmacol. 36, 118–131.

Baek, J.M., Kim, J.-Y., Jung, Y., Moon, S.-H., Choi, M.K., Kim, S.H., Lee, M.S., Kim, I., Oh, J., 2015. Mollugin from Rubea cordifolia suppresses receptor activator of nuclear factor-og ligand-induced osteoclastogenesis and bone resorbing activity in vitro and prevents lipopolysaccharide-induced bone loss in vivo. Phytomedicine 22, 27–35.

Bhattarai, G., Poudel, S.B., Kook, S.H., Lee, J.C., 2017. Anti-inflammatory, anti-osteoclastic, and antioxidant activities of genistein protect against alveolar bone loss and periodontal tissue degradation in a mouse model of periodontitis. J. Biomed. Mater. Res. A 105, 2510–2521.

Billingham, M.E., Morley, J., Hanson, J.M., Shipolini, R.A., Vernon, C.A., 1973. Letter: an anti-inflammatory peptide from bee venom. Nature 245, 163–164.

Bougas, K., Ransjo, M., Johansson, A., 2013. Effects of Porphyromonas gingivalis surface-associated material on osteoclast formation. Odontology 101, 140–149.

Boyce, B., 2013. Advances in the regulation of osteoclasts and osteoclast functions. J. Dent. Res. 92, 860–867.

Boyle, W.J., Simonet, W.S., Lacey, D.L., 2003. Osteoclast differentiation and activation. Nature 423, 337.

Choi, H.J., Park, Y.R., Nepal, M., Choi, B.Y., Cho, N.P., Choi, S.H., Heo, S.R., Kim, H.S., Yang, M.S., Soh, Y., 2010. Inhibition of osteoclastogenic differentiation by Ikarisoside A in RAW 264.7 cells via JNK and NF-kappaB signaling pathways. Eur. J. Pharmacol. 636, 28–35.

Cochran, D.L., 2008a. Inflammation and bone loss in periodontal disease. J. Periodontol. 79, 1569–1576.

Cochran, D.L., 2008b. Inflammation and bone loss in periodontal disease. J. Periodontol. 79, 1569–1576.

Cremasco, V., Decker, C.E., Stumpo, D., Blackshear, P.J., Nakayama, K.I., Nakayama, K., Lupu, T.S., Graham, D.B., Novack, D.V., Faccio, R., 2012. Protein kinase C-delta deficiency perturbs bone homeostasis by selective uncoupling of cathepsin K secretion and ruffled border formation in osteoclasts. J. Bone Miner. Res.: Offic. J. Am. Soc. Bone Miner. Res. 27, 2452–2463.

Cutler, C.W., Kalmar, J.R., Genco, C.A., 1995. Pathogenic strategies of the oral anaerobe, Porphyromonas gingivalis. Trends Microbiol. 3, 45–51.

Dombrowski, Y., Peric, M., Koglin, S., Kaymakanov, N., Schmezer, V., Reinholz, M., Ruzicka, T., Schauber, J., 2012. Honey bee (Apis mellifera) venom induces AIM2 inflammasome activation in human keratinocytes. Allergy 67, 1400–1407.

Fuller, K., Lawrence, K.M., Ross, J.L., Grabowska, U.B., Shiroo, M., Samuelsson, B., Chambers, T.J., 2008. Cathepsin K inhibitors prevent matrix-derived growth factor degradation by human osteoclasts. Bone 42, 200–211.

Garlet, G.P., 2010. Destructive and protective roles of cytokines in periodontitis: a re-appraisal from host defense and tissue destruction viewpoints. J. Dent. Res. 89, 1349–1363.

Geissmann, F., Manz, M.G., Jung, S., Sieweke, M.H., Merad, M., Ley, K., 2010. Development of monocytes, macrophages, and dendritic cells. Science 327, 656–661.

Habermann, E., 1972. Bee and wasp venoms. Science 177, 314–322.

Haffajee, A.D., Socransky, S.S., 1994. Microbial etiological agents of destructive periodontal diseases. Periodontology 5, 78–111 2000.

Hajishengallis, G., 2014. Immunomicrobial pathogenesis of periodontitis: keystones, pathobionts, and host response. Trends Immunol. 35, 3–11.

Halleen, J.M., Raisanen, S., Salo, J.J., Reddy, S.V., Roodman, G.D., Hentunen, T.A., Lehenkari, P.P., Kaija, H., Vihko, P., Vaananen, H.K., 1999. Intracellular fragmentation of bone resorption products by reactive oxygen species generated by osteoclastic tartrate-resistant acid phosphatase. J. Biol. Chem. 274, 22907–22910.

Han, S.M., Kim, J.M., Hong, I.P., Woo, S.O., Kim, S.G., Jang, H.R., Pak, S.C., 2016. Antibacterial activity and antibiotic-enhancing effects of honeybee venom against methicillin-resistant Staphylococcus aureus. Molecules 21, 79.

Han, X., Lin, X., Yu, X., Lin, J., Kawai, T., LaRosa, K.B., Taubman, M.A., 2013. Porphyromonas gingivalis infection-associated periodontal bone resorption is dependent on receptor activator of NF-kappaB ligand. Infect. Immun. 81, 1502–1509.

Hider, R.C., 1988. Honeybee venom: a rich source of pharmacologically active peptides. Endeavour 12, 60–65.

Holt, S.C., Kesavalu, L., Walker, S., Genco, C.A., 1999. Virulence factors of Porphyromonas gingivalis. Periodontology 20, 168–238 2000.

Hotokezaka, H., Sakai, E., Kanaoka, K., Saito, K., Matsuo, K., Kitaura, H., Yoshida, N., Nakayama, K., 2002. U0126 and PD98059, specific inhibitors of MEK, accelerate differentiation of RAW264.7 cells into osteoclast-like cells. J. Biol. Chem. 277, 47366–47372.

Ip, S.-W., Liao, S.-S., Lin, S.-Y., Lin, J.-P., Yang, J.-S., Lin, M.-L., Chen, G.-W., Lu, H.-F., Lin, M.-W., Han, S.-M., 2008. The role of mitochondria in bee venom-induced apoptosis in human breast cancer MCF7 cells. In Vivo 22, 237–245.

Ishibashi, O., Niwa, S., Kadoyama, K., Inui, T., 2006. MMP-9 antisense oligodeoxynucleotide exerts an inhibitory effect on osteoclastic bone resorption by suppressing cell migration. Life Sci. 79, 1657–1660.

Kim, H.K., Kim, M.G., Leem, K.H., 2013. Osteogenic activity of collagen peptide via ERK/MAPK pathway mediated boosting of collagen synthesis and its therapeutic efficacy in osteoporotic bone by back-scattered electron imaging and microarchitecture analysis. Molecules 18, 15474–15489.

Kim, J.H., Kim, E.Y., Lee, B., Min, J.H., Song, D.U., Lim, J.M., Eom, J.W., Yeom, M., Jung, H.S., Sohn, Y., 2016a. The effects of Lycii Radicis Cortex on RANKL-induced osteoclast differentiation and activation in RAW 264.7 cells. Int. J. Mol. Med. 37, 649–658.

Kim, J.Y., Cheon, Y.H., Yoon, K.H., Lee, M.S., Oh, J., 2014. Parthenolide inhibits osteoclast differentiation and bone resorbing activity by down-regulation of NFATc1 induction and c-Fos stability, during RANKL-mediated osteoclastogenesis. BMB Reports 47, 451–456.

Kim, J.Y., Lee, W.R., Kim, K.H., An, H.J., Chang, Y.C., Han, S.M., Park, Y.Y., Pak, S.C., Park, K.K., 2015. Effects of bee venom against Propionibacterium acnes-induced inflammation in human keratinocytes and monocytes. Int. J. Mol. Med. 35, 1651–1656.

Kim, W.H., An, H.J., Kim, J.Y., Gwon, M.G., Gu, H., Park, J.B., Sung, W.J., Kwon, Y.C., Park, K.D., Han, S.M., Park, K.K., 2016b. Bee venom inhibits Porphyromonas gingivalis lipopolysaccharides-induced pro-inflammatory cytokines through suppression of NF-kappaB and AP-1 signaling pathways. Molecules 21.

Kobayashi, N., Kadono, Y., Naito, A., Matsumoto, K., Yamamoto, T., Tanaka, S., Inoue, J., 2001. Segregation of TRAF6-mediated signaling pathways clarifies its role in osteoclastogenesis. EMBO J. 20, 1271–1280.

Kong, X., Wu, W., Yang, Y., Wan, H., Li, X., Zhong, M., Zhao, H., Su, X., Jia, S., Ju, D., Lin, N., 2015. Total saponin from Anemone flaccida Fr. Schmidt abrogates osteoclast differentiation and bone resorption via the inhibition of RANKL-induced NF-kappaB, JNK and p38 MAPKs activation. J. Transl. Med. 13, 91.

Kwon, Y.B., Lee, H.J., Han, H.J., Mar, W.C., Kang, S.K., Yoon, O.B., Beitz, A.J., Lee, J.H., 2002. The water-soluble fraction of bee venom produces antinociceptive and anti-inflammatory effects on rheumatoid arthritis in rats. Life Sci. 71, 191–204.

Kwon, Y.B., Lee, J.D., Lee, H.J., Han, H.J., Mar, W.C., Kang, S.K., Beitz, A.J., Lee, J.H., 2001. Bee venom injection into an acupuncture point reduces arthritis associated edema and nociceptive responses. Pain 90, 271–280.

Lacey, D., Timms, E., Tan, H.-L., Kelley, M., Dunstan, C., Burgess, T., Elliott, R., Colombero, A., Elliott, G., Scully, S., 1998. Osteoprotegerin ligand is a cytokine that regulates osteoclast differentiation and activation. Cell 93, 165–176.

Lee, W.R., Pak, S.C., Park, K.K., 2015. The protective effect of bee venom on fibrosis causing inflammatory diseases. Toxins 7, 4758–4772.

Lee, W.R., Park, J.H., Kim, K.H., Park, Y.Y., Han, S.M., Park, K.K., 2011. Protective effects of melittin on transforming growth factor-beta 1 injury to hepatocytes via anti-apoptotic mechanism. Toxicol. Appl. Pharmacol. 256, 209–215.

Li, C.H., Amar, S., 2007. Morphometric, histomorphometric, and microcomputed tomographic analysis of periodontal inflammatory lesions in a murine model. J. Periodontol. 78, 1120–1128.

Li, C.Y., Jepsen, K.J., Majeska, R.J., Zhang, J., Ni, R., Gelb, B.D., Schaffler, M.B., 2006. Mice lacking cathepsin K maintain bone remodeling but develop bone fragility despite high bone mass. J. Bone Miner. Res. : Offic. J. Am. Soc. Bone Miner. Res. 21, 865–875.

Liu, Y.C., Lerner, U.H., Teng, Y.T., 2010a. Cytokine responses against periodontal infection: protective and destructive roles. Periodontology 52, 163–206 2000.

Liu, Y.C.G., Lerner, U.H., Teng, Y.T.A., 2010b. Cytokine responses against periodontal infection: protective and destructive roles. Periodontology 52, 163–206 2000.

Matsumoto, M., Sudo, T., Saito, T., Osada, H., Tsujimoto, M., 2000. Involvement of p38 mitogen-activated protein kinase signaling pathway in osteoclastogenesis mediated by receptor activator of NF-kappa B ligand (RANKL). J. Biol. Chem. 275, 31155–31161.

Matsuo, K., Galson, D.L., Zhao, C., Peng, L., Laplace, C., Wang, K.Z., Bachler, M.A., Amano, H., Aburatani, H., Ishikawa, H., Wagner, E.F., 2004. Nuclear factor of activated T-cells (NFAT) rescues osteoclastogenesis in precursors lacking c-Fos. J. Biol. Chem. 279, 26475–26480.

Mau, L.-P., Cheng, W.-C., Chen, J.-K., Shieh, Y.-S., Cochran, D.L., Huang, R.-Y., 2016. Curcumin ameliorates alveolar bone destruction of experimental periodontitis by modulating osteoclast differentiation, activation and function. J. Func. Foods 22, 243–256.

Nakamura, I., Duong, L.T., Rodan, S.B., Rodan, G.A., 2007a. Involvement of alpha(v) beta3 integrins in osteoclast function. J. Bone Miner. Metab. 25, 337–344.

Nakamura, I., Duong, L.T., Rodan, S.B., Rodan, G.A., 2007b. Involvement of alpha(v) beta3 integrins in osteoclast function. J. Bone Miner. Metab. 25, 337–344 (iodontitis by).

Orsolic, N., 2012. Bee venom in cancer therapy. Cancer Metastasis Rev. 31, 173–194.

Park, M.H., Choi, M.S., Kwak, D.H., Oh, K.W., Yoon, D.Y., Han, S.B., Song, H.S., Song, M.J., Hong, J.T., 2011. Anti-cancer Effect of Bee Venom in Prostate Cancer Cells through Activation of Caspase Pathway via Inactivation of NF-κancer Effect of Bee Venom in.

Pizzo, G., Guiglia, R., Lo Russo, L., Campisi, G., 2010. Dentistry and internal medicine: from the focal infection theory to the periodontal medicine concept. Eur. J. Intern. Med. 21, 496–502.

Sakellari, D., Menti, S., Konstantinidis, A., 2008. Free soluble receptor activator of nuclear factor-kappab ligand in gingival crevicular fluid correlates with distinct pathogens in periodontitis patients. J. Clin. Periodontol. 35, 938–943.

Son, D.J., Lee, J.W., Lee, Y.H., Song, H.S., Lee, C.K., Hong, J.T., 2007. Therapeutic application of anti-arthritis, pain-releasing, and anti-cancer effects of bee venom and its constituent compounds. Pharmacol. Ther. 115, 246–270.

Stieger, M., Wuthrich, B., Wyss, S., Kopper, E., 1978. [Clinical picture and diagnosis of bee-venom allergy. A comparison between skin tests and RAST determinations].

Hautarzt 29, 632–637.
Sui, X., Kong, N., Ye, L., Han, W., Zhou, J., Zhang, Q., He, C., Pan, H., 2014. p38 and JNK MAPK pathways control the balance of apoptosis and autophagy in response to chemotherapeutic agents. Cancer Lett. 344, 174–179.
Taguchi, H., Aono, Y., Kawato, T., Asano, M., Shimizu, N., Saigusa, T., 2015. Intragingival injection of Porphyromonas gingivalis-derived lipopolysaccharide induces a transient increase in gingival tumour necrosis factor-alpha, but not interleukin-6, in anaesthetised rats. Int. J. Oral Sci. 7, 155–160.
Takayanagi, H., Kim, S., Matsuo, K., Suzuki, H., Suzuki, T., Sato, K., Yokochi, T., Oda, H., Nakamura, K., Ida, N., 2002. RANKL maintains bone homeostasis through c-Fos-dependent induction of interferon-β. Nature 416, 744.
Thummuri, D., Jeengar, M.K., Shrivastava, S., Nemani, H., Ramavat, R.N., Chaudhari, P., Naidu, V.G., 2015. Thymoquinone prevents RANKL-induced osteoclastogenesis activation and osteolysis in an in vivo model of inflammation by suppressing NF-KB and MAPK Signalling. Pharmacol. Res. 99, 63–73.
Turk, V., Stoka, V., Vasiljeva, O., Renko, M., Sun, T., Turk, B., Turk, D., 2012. Cysteine cathepsins: from structure, function and regulation to new frontiers. Biochim. Biophys. Acta 1824, 68–88.
Väänänen, H.K., Horton, M., 1995. The osteoclast clear zone is a specialized cell-extracellular matrix adhesion structure. J. Cell Sci. 108, 2729–2732.
Wara-aswapati, N., Surarit, R., Chayasadom, A., Boch, J.A., Pitiphat, W., 2007. RANKL upregulation associated with periodontitis and Porphyromonas gingivalis. J. Periodontol. 78, 1062–1069.
Wilson, S.R., Peters, C., Saftig, P., Brömme, D., 2009. Cathepsin K activity-dependent regulation of osteoclast actin ring formation and bone resorption. J. Biol. Chem. 284, 2584–2592.
Yagi, M., Miyamoto, T., Sawatani, Y., Iwamoto, K., Hosogane, N., Fujita, N., Morita, K., Ninomiya, K., Suzuki, T., Miyamoto, K., 2005. DC-STAMP is essential for cell–cell fusion in osteoclasts and foreign body giant cells. J. Exp. Med. 202, 345–351.
Zenger, S., Hollberg, K., Ljusberg, J., Norgard, M., Ek-Rylander, B., Kiviranta, R., Andersson, G., 2007. Proteolytic processing and polarized secretion of tartrate-resistant acid phosphatase is altered in a subpopulation of metaphyseal osteoclasts in cathepsin K-deficient mice. Bone 41, 820–832.
Zhang, C., Dou, C.E., Xu, J., Dong, S., 2014a. DC-STAMP, the key fusion-mediating molecule in osteoclastogenesis. J. Cell. Physiol. 229, 1330–1335.
Zhang, W., Ju, J., Rigney, T., Tribble, G., 2014b. Porphyromonas gingivalis infection increases osteoclastic bone resorption and osteoblastic bone formation in a periodontitis mouse model. BMC Oral Health 14, 89.
Zhao, Q., Wang, X., Liu, Y., He, A., Jia, R., 2010. NFATc1: functions in osteoclasts. Int. J. Biochem. Cell Biol. 42, 576–579.
Zhou, Q., Desta, T., Fenton, M., Graves, D.T., Amar, S., 2005. Cytokine profiling of macrophages exposed to Porphyromonas gingivalis, its lipopolysaccharide, or its FimA protein. Infect. Immun. 73, 935–943.